Processing of Plant Fiber Composites by Liquid Molding Techniques: An Overview

Gaston Francucci, Exequiel Rodriguez
Composite Materials Group (CoMP), Research Institute of Material Science and Technology, INTEMA-CONICET, Engineering Faculty, National University of Mar del Plata, B7608FDQ Mar del Plata, Argentina

Lately, researchers around the world have developed effective chemical and physical treatments on plant fibers to improve their compatibility with polymeric matrices. In addition, the need of high performance fabrics produced from plant fibers has been addressed by many manufacturers of textile reinforcements. These facts have increased the use of natural fibers in the composite industry. Liquid Composite Molding (LCM) techniques are suitable for mass production of high-quality composite parts. Basically, the reinforcement is compressed inside a mold and a thermosetting resin is injected to impregnate the fibers and fill the empty spaces in the mold. After the resin cures, the composite part is demolded. However, the processing of plant fiber–reinforced composites by the traditional techniques is not trivial, because the structure of plant fibers is more complex than that of synthetic fibers and due to their chemical composition rich in cellulose and hemicellulose, they are highly hydrophilic. This work presents a review on the main issues that arise during the processing of plant fiber reinforced composites by traditional liquid composite molding techniques. POLYM. COMPOS., 00:000–000, 2014. © 2014 Society of Plastics Engineers

BIOCOMPOSITES

Nowadays, the increasing environmental pollution and the reduction of nonrenewable resources have led industry and academia to focus their research on the development of materials that are environment friendly and made from renewable resources. In this context, bio composites are being created using natural fibers in conjunction with bioresins. In some cases, because of different factors (insufficient properties of one of the components, limited supply, high cost, high moisture absorption, etc.), hybrid composites are made with natural fibers and polymeric matrices derived from the petrochemical industry or vice versa.

Natural fibers can be classified according to the origin as plant, mineral and animal fibers. Plant fibers have the higher potential as reinforcement for composite materials due to their superior stiffness, strength and availability [1]. These fibers can be extracted from different parts of the plant such as [2]: the bast fibers (jute, kenaf, hemp, ramie, flax), leaf fibers (sisal), fruit fibers (coconut), seed fibers (cotton), straw fibers, and grass fibers. The microstructure of plant fibers is extremely complex due to the hierarchical organization at different length scale and the different materials present in variable proportions. Plant fibers essentially consist of two cell walls arranged as concentric cylinders with a small channel in the middle called the lumen [3]. The bulk of the fiber is essentially constituted by the layer S2 of the secondary wall cell. The main chemical constituent of the fiber cell wall is cellulose, which chains are arranged in parallel to form bundles, denoted microfibrils, which are usually bonded together with lignin, pectin and hemicellulose. The structure of the cell wall is organized into a number of layers differing by the angle of the cellulose microfibrils to the longitudinal fiber axis. Thus, the cell wall of plant fibers is organized like a composite laminate with a number of layers with differently oriented, stiff and strong semicrystalline cellulose microfibrils embedded in a matrix of hemicellulose, pectin, and lignin. Figure 1a shows the structure of an elementary fiber, and Fig. 1b shows a SEM image of a jute fiber. It can be seen that a single fiber is composed of several elementary fibers linked together by pectins. Due to their chemical composition rich in cellulose (Table 1), plant fibers are highly hydrophilic. Table 2 presents physical and mechanical properties of some plant fibers and glass fibers.

The environmental advantages of plant fibers have been demonstrated by many studies of sustainability and life cycle assessments [12–16]. In addition, these fibers are renewable, abundant and cheaper than synthetic ones; they are less abrasive, which reduces wearing of tools and the health risk to workers and operators; they have good thermal and acoustic insulation properties, low density and good specific properties [17]. On the other hand, plant fibers have some limitations, such as water absorption [18, 19] that can result in swelling of the fibers,

Correspondence to: Gaston Francucci; e-mail: gfrancucci@fi.mdp.edu.ar
DOI 10.1002/pc.23229
Published online in Wiley Online Library (wileyonlinelibrary.com).

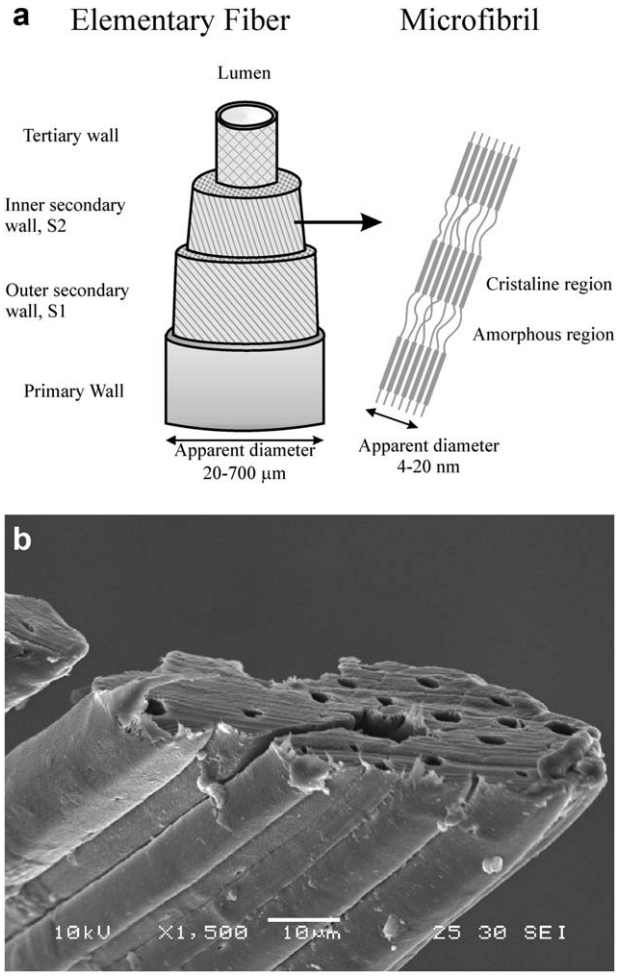

FIG. 1. (a) Schematic representation of a plant fiber. (b) SEM image of a jute fiber.

which in turn can reduce the dimensional stability of the agro-fiber composites, and also deteriorates their mechanical properties as it weakens the matrix–fiber interface. Other drawback of these fibers is their low thermal stability, because they suffer lignocellulosic degradation at low temperatures (about 200°C), limiting their use in some applications and also the processing temperatures [20]. Furthermore, their mechanical properties are lower than those of glass and carbon fibers, and their chemical compatibility with most polymeric matrices is also inferior, resulting in lower mechanical performance of the composites. Another disadvantage of plant fibers is the great variability in physical and mechanical properties found among fibers of the same type (Table 2), depending on climatological and geographic conditions during plant growth [21].

REINFORCEMENTS MADE FROM PLANT FIBERS

There are some characteristics of plant fiber fabrics that should be considered if traditional processing techniques are to be used to manufacture green composite parts:

- Reinforcements made of plant fibers are prone to exhibit significant inconsistency in properties such as surface density, fiber and yarn dimensions and fiber chemical composition, depending on the plant growing conditions.
- Continuous filament bundles are impossible to obtain with plant fibers. Fiber length can vary from several millimeters to a few meters. Different methods are used to make large rovings from short fibers. Usually, continuous rovings are made with short twisted fibers, as shown in Fig. 2a. On the other hand, glass fiber rovings are continuous filament bundles, as shown in Fig. 2b.
- Due to their hydrophilic nature, plant fiber based reinforcements usually contain around 10% of absorbed water in the fiber micro structure. Water can interfere with the polymerization reaction, degrade the fiber-matrix interface and generate voids in the composite microstructure. Therefore it is highly recommended to dry the fabrics and decrease water content to 2 to 3% before the processing of the materials [22].
- Thermal stability of the fibers must be considered when using high processing temperatures. This is a very important issue in most thermoplastics processing techniques, but it is not critical when thermosetting matrices are used, since a wide variety of them can be cured at safe temperatures.

PROCESSING OF PLANT FIBER COMPOSITES

Thermosetting matrix composite parts can be manufactured by several techniques such as hand lay-up, liquid compression molding, filament winding, pultrusion, autoclave processing and liquid composite molding techniques. The most used processing techniques for the production of composite parts based on natural fibers and

TABLE 1. Chemical composition of some vegetable fibers [4–7].

Fiber type	Cellulose (%)	Lignin (%)	Hemicellulose (%)	Pectin (%)	Wax (%)	Moisture (%)
Jute	51–72	5–13.0	12–20.4	0.2	0.5	10
Flax	60–81	2–3	14–18.6	1.8–2.3	1.3–1.5	10
Hemp	70–78	3.7–5	17.9–22	0.9	0.7	10
Ramie	68.6–76	0.6–1	13.1–15	1.9–2	0.3	10
Kenaf	36	18	21	2	–	–
Sisal	43–88	4–12	10–13	0.8–2	0.3	10
Henequen	60–78	8–13	4–28	3–4	–	–
Cotton	82.7–92	0–1	2–5.7	5.7	0.6	10

DOI 10.1002/pc

TABLE 2. Properties of some vegetable fibers compared to those of glass fibers [8–11].

	Fiber					
Property	E-Glass	S-Glass	Flax	Hemp	Jute	Sisal
Density (g/cm^3)	2.55	2.49	1.4–1.5	1.4–1.5	1.3–1.46	1.4–1.45
Tensile strength (MPa)	3450	4300	345–1500	310–1834	350–900	511–635
Young modulus (GPa)	72.4	86.9	50–110	35–70	10–30	9.4–22
Elongation (%)	4.8	5	1.2–3.3	1.6–3	1.2–1.8	2–2.5
Specific tensile strength (MPa* cm^3/g)	1353	1727	238–1000	214–1264	286–650	360–447
Specific young modulus (GPa* cm^3/g)	28	35	34–76	24–50	7–22	7–15

thermosetting polymer matrices used to be hand lay-up and compression molding due to the low costs associated to these methods [23], but nowadays the spotlight is right on the liquid composite molding (LCM) techniques because these are automated processes that offer short processing cycles, high product quality and enables mass production [24]. Although autoclave processing of bio composites is possible, it is not common because it is a very expensive technique and bio composites are not meant to be used in high performance applications. Therefore, and since the hand lay-up and compression molding processes require little scientific attention, this review presents the recent findings on the issues that arise during the processing of plant fiber composites by LCM techniques. Pultrusion and filament winding techniques are not specifically treated in this article, but many of the conclusions made for LCM techniques can be extrapolated to those processes.

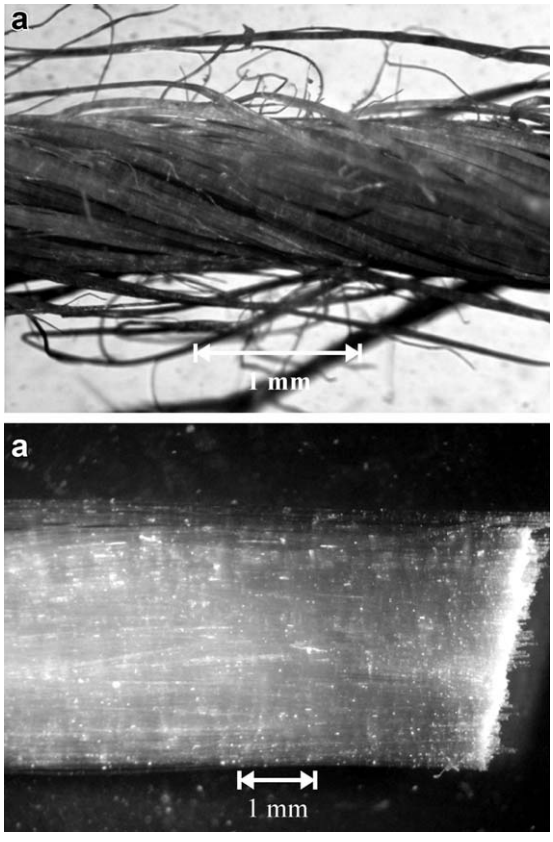

FIG. 2. (a) Jute fiber bundle extracted from a bidirectional woven fabric. (b) Glass fiber bundle.

The first step in most of LCM techniques is the preparation of the preform by cutting and stacking several layers of the fabric or mat used as reinforcement. Sometimes fabric orientation is changed from layer to layer in order to modify the isotropy of the composite. Usually a pre-forming step is done prior to place the fabrics in the mold. This step consists in compressing a stack of fabric layers in a mold to a shape and thickness close to those of the final part. A binder is sometimes used to avoid preform deformation during handling. Afterwards the preform is placed inside a mold that closes compressing the preform to the desired thickness, which in turn determines the final fiber volume fraction of the composite. Then, a catalyzed resin is forced to flow through the dry preform and the reinforcement is impregnated by the resin. After the mold is completely filled, the resin is left to cure (usually assisted by a heated mold) and after reaching the desired degree of cure, the part can be removed from the mold and the cycle is repeated.

There are many different liquid composite molding processes, which are described in Table 3. Some of these processes involve two rigid mold halves (RTM, LRTM, ICM) while others use a flexible sheet as the upper mold half. The most widely used LCM process for low volume production of large parts is Vacuum Infusion (VI). In this process (Fig. 3a), the preform is placed on a rigid lower side of the mold and resin and vacuum lines are strategically positioned over the preform. A flexible sheet or reusable bag is positioned on top of it and sealed to the lower side of the mold, and vacuum is applied to compact the reinforcement and eliminate air. Finally, resin lines are opened and it is introduced as the vacuum draws it through the reinforcement. This technique, which is widely used to produce very large parts, has some disadvantages such as: poor surface finish in the side of the bag, low available compaction and injection pressure (1 atm), long cycle times and wastage of large amounts of disposable materials such as the vacuum bags, peel ply

TABLE 3. Some liquid composite molding processes.

Process	Initials	Tooling	Production volume	Part complexity	Part size
Resin Transfer Molding	RTM	Rigid mold (steel or aluminum)	High	High	Small–medium
Light Resin Transfer Molding	LRTM	Rigid mold (glass fiber reinforced composites)	Low-Medium	Medium	Small-medium
Vacuum Infusion	VI	Rigid lower mold—flexible sheet (vacuum bag, plastic sheet, silicone or rubber membrane)	Low	Medium	Medium-large
Injection Compression Molding	ICM	Rigid mold (steel or aluminum)	Medium-high	Medium	Small-medium

and hoses. On the other hand, Resin Transfer Molding (RTM) is the most used technique for mass production of complex parts. In this process (Fig. 3b) both sides of the mold are rigid, usually made of steel and resin is introduced via a pumping mechanism. The higher injection pressures used in this technique give more flexibility in types of resins and fillers, and allow obtaining higher fiber contents. Other benefits are better cosmetic finishes, lower variation in part thickness, and faster cycle times. Light Resin Transfer Molding is (LRTM) a variant for RTM that is widely used for low to medium volume applications. LRTM tooling costs are a fraction of the price of equivalent RTM molds but also the production rate is lower. The closed mold consists of an "A" side mold (base mold) and a semi-rigid "B" side mold (counter mold) that is sealed to the "A" side mold using vacuum pressure. Flexibility of the counter mold enables it to fit perfectly with the base mold, which is essential to achieving the necessary vacuum pressures and precision parts. Resin is drawn into the resulting cavity under vacuum. The resin infusion may be assisted by a resin injection pump, which will accelerate the infusion process. Another LCM variant is Injection Compression Molding (ICM), which involves a compression stage of a preform that has already been saturated with the resin. In this process, the preform is placed in the mold and an initial compression stage is performed with the mold remaining partially open. Resin is introduced into the mold cavity through injection gates until the required volume of resin has been injected. At this point all injection gates are closed, and the mold platens are brought together driving the resin through the remaining dry areas of the preform and compressing the laminate to the final cavity thickness.

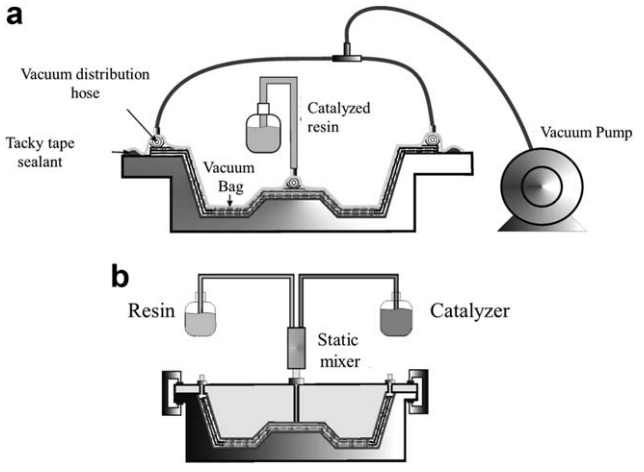

FIG. 3. (a) Vacuum infusion set up. (b) Resin transfer molding set up.

The two critical stages occurring during the LCM processing are the compaction and impregnation of the preform, which will be explained in detail in the following sections.

COMPACTION OF PLANT FIBER PREFORMS

The compaction response of fibrous preforms determines the maximum fiber content that can be achieved with the available clamping forces. This is very important in single-sided molding processes like VI, where the maximum compaction pressure is limited to the atmospheric pressure. It should be taken into account that in general, the higher the fiber volume fraction of a composite is, the higher its performance is. Moreover, higher fiber contents will result in more ecofriendly composites when petrochemical resins are reinforced with natural fibers, since the percentage of materials from renewable sources is increased [25]. Besides the maximum compaction pressures needed to achieve a certain fiber volume fraction, the other properties that characterize the compaction behavior of fibrous preforms are the permanent deformation after subsequent loading cycles [26, 27] and the stress relaxation that occurs while the desired thickness is kept constant [28–30]. The permanent deformation of synthetic woven preforms is usually attributed to the irreversible yarn cross section deformation, flattening, and nesting; while in random mats permanent deformation is caused by the filaments from one layer of fabric that are intertwined or embedded in the adjoining layer. Preforms that experience high permanent deformation are easier to place in the mold after the preforming stage and, because it thickness is closer to the final part thickness, the required clamping forces are lower. In the same way, a higher fiber volume fraction can be obtained after a preforming step in single-sided molding processes such as VI. Stress relaxation means that the load required for maintaining a fixed thickness in a preform decreases with

 DOI 10.1002/pc

time. In the same way, if a constant load is applied to a preform as it happens in vacuum infusion technique, its thickness will decrease with time. This phenomenon is known as fiber settling.

Some LCM processes, such as ICM, involve a compression stage of a preform that has already been saturated with the resin. Two opposite effects occur during the compaction stage in the presence of a fluid. The fluid acts as a lubricant and reduces the clamping forces needed to achieve the desired volume fraction. On the other hand, an internal fluid pressure is generated as the compaction plate descends and the fluid is drained through the preform [28–31] which increases the clamping forces. The effect of the fluid (resin) on the compaction response of reinforcements is also important in single sided molding processes like VI. In these cases, the fluid lubricates the fibers reducing inter fiber friction and allowing the vacuum bag to compress the preform to a lower thickness. Nevertheless, a linear pressure gradient is expected to develop from the resin inlet gate (pressure = atmospheric pressure) towards the vacuum outlet gate (pressure = 0). This pressure buildup throughout the wet area of the preform reduces the effective compaction pressure given by the atmosphere pushing on the vacuum bag, increasing the thickness of the wet laminate.

However, many LCM processes comprise compaction step of dry fibrous preforms. Almost all the authors that have studied the compaction of plant fiber preforms agreed that they are more difficult to compress than preforms made of glass fiber fabrics [31–35], in contrast to what could be expected considering that the stiffness of plant fibers is lower than the stiffness of glass fibers. This means that higher clamping forces will be required to achieve a certain fiber volume fraction, or lower fiber content will be achieved with the available clamping force. Authors attributed the difference in compaction behavior between glass and plant fiber preforms to the rough surface of these fibers that leads to large interfiber friction forces, increasing the compaction pressure needed to reach high fiber contents. In addition, they suggested that because many plant fibers are actually discontinuous fibers twisted around each other and bundles are usually made of short twisted fibers, the degree of misalignment is high causing the compaction to be harder.

Table 4 presents compaction data found by different authors for dry natural fiber preforms, showing the fiber content that would be obtained if the vacuum infusion process is used and the clamping pressures that would be needed to achieve different fiber volume fractions. Results show that natural fiber vacuum infused composites will usually have low fiber contents and therefore, poor mechanical properties. Rigid mold techniques are therefore most suitable to produce high performance (and more environmentally friendly) components. In addition, Light RTM would be more appropriate than RTM if production costs are considered in the selection of the processing technique, because it requires less-expensive tooling. RTM molds are more expensive and should only be preferred for more valuable composites.

Another peculiarity of the compaction behavior of plant fiber fabrics is the high permanent deformation that occurs after one or more compressive loading cycles, several times higher than the permanent deformation reported for glass fiber fabrics with similar architecture [32, 33, 35–38]. This means that the difference between the first and second compaction curves is larger in natural fiber preforms than in the case of glass fiber preforms. Authors suggested that plant fiber cell walls collapse and the lumens are closed in an irreversible manner when compressive forces are applied to the preform. These phenomena were found to be more significant when the fiber content (and transverse deformation) was increased [33]. In addition, plastic deformation of plant fibers was confirmed by Poilâne et al. [39] during mechanical testing of flax/epoxy composites. Table 5 shows some reported values for permanent deformation observed after the first loading cycle carried out on preforms compressed to different final thicknesses or fiber contents.

The significant permanent deformation observed in these natural fiber reinforcements can be used to increase the fiber volume fraction of the composites manufactured by the VI technique, as shown schematically in Fig. 4. Consider P_1 to be equal to 1 atm. If the uncompressed preform is compacted by the vacuum bag with P_1 a fiber volume fraction of V_{F1} would be obtained. If a first loading cycle such as the one shown in the figure is applied compressing the preform with a pressure P_2, the second loading cycle would be shifted to higher values of fiber content due to the permanent deformation experienced by the preform. Therefore, compressing the preform with the atmospheric pressure P_1 during the second loading cycle would lead now to higher fiber content, V_{F2}. It should be taken into account that increasing the maximum pressure reached in the first cycle will increase displacement in the second loading cycle and will allow obtaining higher fiber contents in the VI technique [36]. In addition, the difference observed between the first and second loading cycles is much more significant than the one observed between the second and successive loading cycles [36].

Significant stress relaxation was found to occur in hemp and flax mats by Khoun et al. [32], in jute woven fabrics and sisal mats by Francucci et al. [33] and in wood fiber mats manufactured by different techniques by Umer et al. [31, 37]. Some reported values for stress relaxation are given in Table 5.

One interesting fact found by Francucci et al. [33] was that glass fiber random mats experienced larger stress relaxation when compressed dry than when compressed in the presence of a polar test fluid (20% water/glycerin solution), while sisal and jute fiber preforms responded in the opposite manner. The lubrication effect was expected to decrease the amount of stress relaxation, because fiber realignment and reorientation and the interactions between consecutive layers are enhanced during the compaction

TABLE 4. Compressibility of some vegetable fiber fabrics and mats.

Fiber/Fabric	Compaction speed (mm/min)	Volumetric fiber content (%) obtained with a compaction pressure of 1 atm (0.1013 MPa)	Compaction pressure needed to obtain different fiber volume fractions (MPa)				Refs.
			$V_F = 0.2$	$V_F = 0.3$	$V_F = 0.4$	$V_F = 0.5$	
Jute/Woven fabrics 330g/m^2	0.5	27	0.006	0.19	0.65	1.33	36
	5	26	0.010	0.20	0.69	1.35	
	50	25	0.015	0.27	0.8	1.55	
Flax/mat, 450g/m^2 (large diameter, short length yarn)	2	24	0.041	0.25	0.84	-	37
Flax/mat, 450g/m^2 (large diameter, long length yarn)	2	23	0.057	0.36	1.19	-	
Flax/mat, 400g/m^2 (small diameter, short length yarn)	2	21	0.09	0.48	1.4	-	
Flax/mat, 400g/m^2 (small diameter, long length yarn)	2	Lower than 20	0.13	0.65	1.86	-	
Hemp/strand mat, 500 g/m^2	50	17	0.17	0.62	1.43	2.57	32
Flax/strand mat, 500 g/m^2		17	0.17	0.62	1.53	2.78	
Wood/random mat (MDF), 2000–2100 g/m^2	0.5	17	0.32	1.68	3.13	-	31
Sisal/random mat, 850 g/m^2	0.5	16	0.270	1.090	-	-	33
Flax/nonwoven mat, 350 g/m^2	2	16	0.25	0.98	2.76	-	35
Wood/random mat (DMF), 350–375 g/m^2	0.5	Lower than 15	0.481	1.27	2.26	-	31
Wood/random mat (HS), 400 g/m^2	0.5		0.69	1.83	3.19		
Wood/random mat (PDF), 400 g/m^2	0.5		0.796	2.04	3.43		
Wood/random mat (PDF), 400 g/m^2	2		0.74	1.94	3.3		34
Wood/random mat (PDF), 400 g/m^2	25		0.84	2.13	3.56		
Hemp/nonwoven mat, 320 g/m^2	2	14	0.37	1.34	3.51		35
Wood/random mat (DMF), 350–375 g/m^2	2	12	0.59	1.51	2.52		34
	25	12	0.52	1.45	2.52		
Jute/nonwoven mat, 230 g/m^2	2	10	0.75	2.66	-		35

stage in the presence of a fluid, and a more stable fiber array is obtained. However, plant fiber fabrics showed an opposite trend, suggesting that the load could have dropped due to fiber softening instead of relaxation processes, decreasing the compaction load measured during the relaxation step.

It is known that for plant fibers, water and other polar substances present in the test fluid will soak into the fiber walls causing dimensional changes and softening [40]. Many authors have found that this affects the compaction response of plant fiber preforms by decreasing the compaction loads required to achieve certain fiber content. Umer et al. [31] performed saturated compaction tests to different wood fiber mats using a water/glucose syrup solution and mineral oil. They observed that water contained in the glucose syrup dramatic softening of the wood fibers. They did not observe any apparent influence on the compaction response of the wood mats when infiltrated with mineral oil. Francucci et al. [33] studied the compaction response of glass fiber mat, sisal fiber mat, and jute woven fabric preforms which were immersed in a water/glycerin solution for different time periods before performing the compaction test. They reported that jute preforms softened as the immersion time was increased up to 15 min. After 15 min of immersion, the compaction behavior reached a steady state, and no further differences were observed. Sisal preforms also softened as the immersion time increased, but the steady state was reached after 60 min of immersion. The total pressure drop was found to be 27% for jute woven fabrics and 10% for sisal mat. The authors did not find any difference among all the compaction curves for the glass fiber mat as the immersion time was increased. Therefore, if water based bioresins are utilized, significant fiber softening will reduce the compaction stress required to achieve a certain volume fraction. Synthetic fibers on the other hand, were found to be unaffected by the type of fluid which will only produce a lubrication effect.

Modeling the Compaction Response of Plant Fiber Reinforcements

The modeling of the compaction stage in LCM is important to obtain analytical expressions which relate the fiber volume fraction with the compaction pressure, as the processing variables (compaction speed, number of loading cycles, etc.) are modified. Many authors proposed suitable models to describe the compaction behavior of synthetic fiber assemblies [41–51]. Theoretical models are based on many geometric assumptions, material idealizations and suppositions about the interaction between fibers and tows. Francucci and Rodríguez [52] explored the different theoretical models found in literature for synthetic fiber preforms and questioned their applicability

 DOI 10.1002/pc

TABLE 5. Permanent deformation and stress relaxation experienced by some vegetable fiber mats and fabrics.

Fiber/fabric	Compaction speed (mm/min)	Final Volumetric Fiber Content (%)	Permanent deformation (%)	Stress relaxation (%)	Refs.
Jute/Woven fabrics 330g/m^2	5	35	22	28.7	36
		45	26	26.5	
		55	31	23.5	
Sisal/random mat. 850 g/m^2	5	35	42	32	33
Hemp/strand mat. 500 g/m^2	50	35	65.5	39	32
		50	69	35	
		65	79	28	
Flax/strand mat. 500 g/m^2		35	62	41	
		50	67	37	
		65	70	29	

in plant fiber fabrics. They concluded that most of the assumptions used by the theoretical models developed in literature for fabrics made of synthetic fibers are not applicable to plant fiber fabrics, because of their hollow structure, rough surface, the high permanent deformation they suffer throughout compaction, the large inhomogeneity of these fabrics and the fiber and bundle complex geometry and assembly. Therefore they suggested the use of empirical models to represent the compaction response of these natural fiber fabrics. Three empirical compaction models were considered by those authors: the power law, the exponential function and the Freundlich model. The first two models represented fairly well the compaction curve of jute fabrics, but the fitting was not perfect, while the latter model fitted almost perfectly the whole compaction curve at all the pressure range. In addition, the authors found that the Freundlich model leaded to a significantly smaller error than the others when they were used to extrapolate the compaction vs. fiber volume fraction curve at higher fiber contents than the ones reached experimentally. Umer et al. [34] fitted the data recorded during the dynamic and static compaction experiments performed on wood fiber preforms to a five term polynomial empirical model, which showed a good fit over a wide range of fiber volume fractions.

Figure 5 shows plots of the mentioned empirical models fitting a typical compaction curve of a jute woven fabric preform (10 fabric layers). The mathematical expression of these models is presented in Table 6. These equations correlate the applied compaction pressure (σ) to the fiber volume fraction (V_F) using different fitting parameters.

Summarizing, the development of theoretical models to predict the compaction behavior of plant fiber fabrics is almost impossible because of the complex structure of the fibers, the large variability on its properties, and the inhomogeneous nature of the fabrics made of natural fibers. Therefore, the use of empirical models is recommended to represent the compaction response of plant fiber fabrics. Among the different models proposed in literature, the Freundlich model and the five term polynomial model are the ones that best fit the experimental data, being the first one more advantageous since it comprises only three fitting parameters.

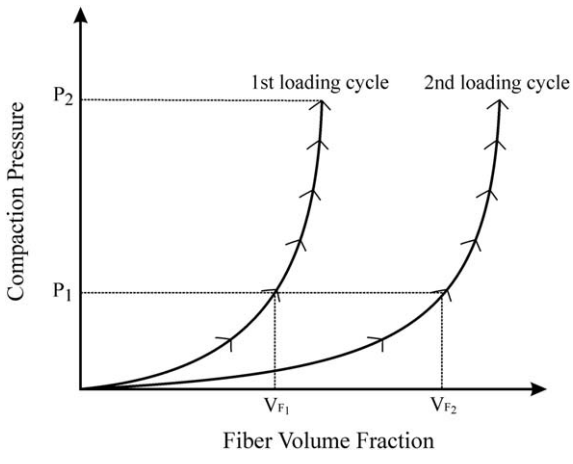

FIG. 4. Compaction curves for the first and second loading cycles.

IMPREGNATION OF PLANT FIBER FABRICS

The correct impregnation of the reinforcements is crucial to obtain composite parts free of defects and with high mechanical properties. Darcy's law is widely used to model the fluid flow through a porous medium, and it is also extensively used in modeling flow processes in composite materials. Darcy's law is shown in *Eq. 1*, where $\overline{u}$ (m/s) is the averaged resin velocity (Darcy's velocity), $\overline{\overline{K}}$ (m^2) is the permeability tensor, η (Pa.s) is the fluid viscosity, and ∇P (Pa/m) is the applied pressure gradient. *Equation 2* shows the one-dimensional form of Darcy's law, taking into account that the Darcy's velocity is related to the superficial fluid velocity, v (which is the observable velocity), through the porosity of the preform, ϕ. According to this law, the fabric property that affects the fluid flow is its permeability, which is considered to be constant and dependent on the fabric architecture, fiber type and porosity of the fiber bed.

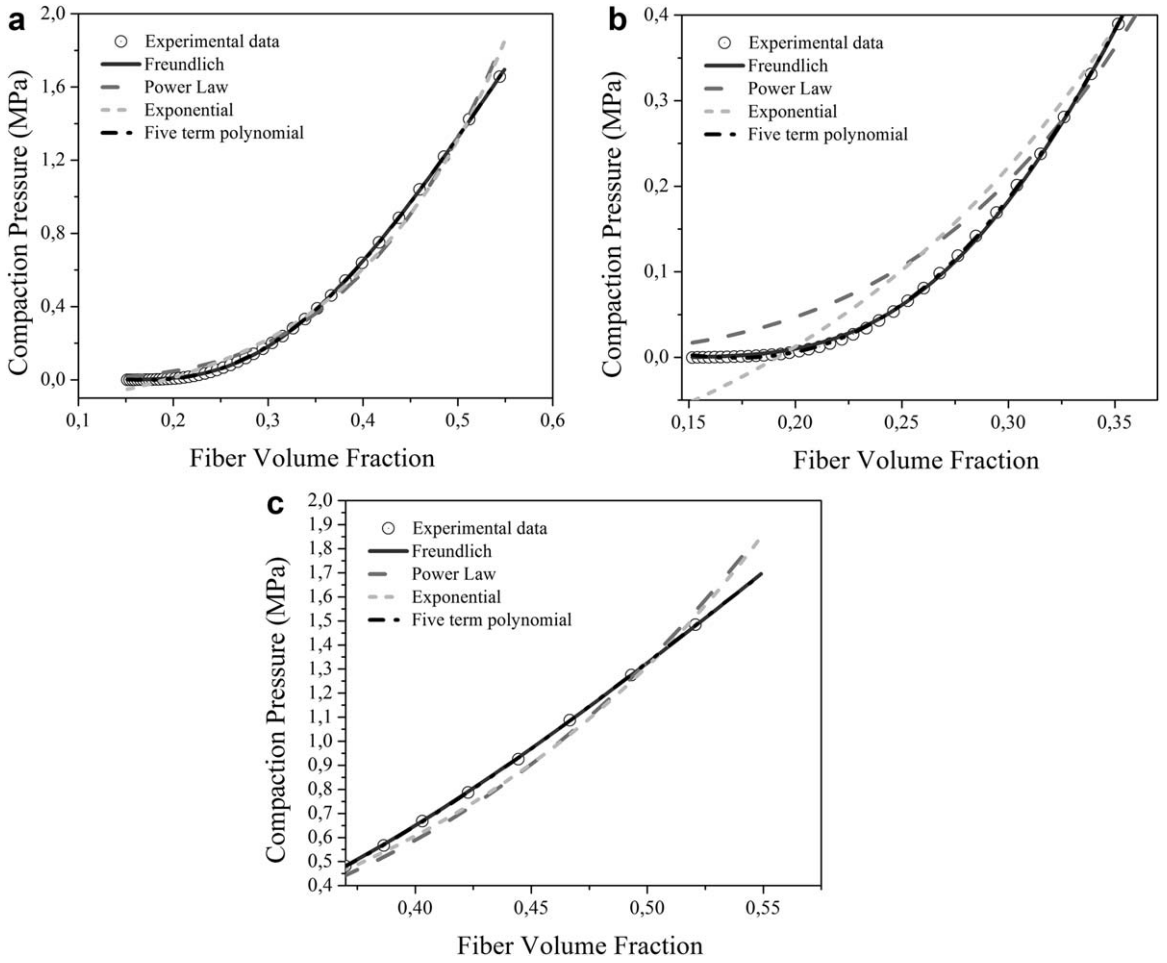

FIG. 5. Empirical compaction models for plant fiber fabrics. (a) Complete fiber content range, (b) low fiber content range, and (c) high fiber content range.

$$\overline{u} = -\frac{\overline{\overline{K}}}{\eta}\nabla P \tag{1}$$

$$v = -\frac{K}{\phi\eta}\frac{\partial P}{\partial x} \tag{2}$$

The modified Carman–Kozeny model is commonly used to establish a relationship between permeability and porosity (defined as: 1—fiber volume fraction) [53, 54]. The expression of the modified Carman–Kozeny model is shown in *Eq. 3*, where n and C are empirical parameters.

$$K = \frac{\phi^{n+1}}{C(1-\phi)^n} \tag{3}$$

High porosities lead to high values of permeability, and make easier the resin flow during impregnation. This enhances fabric impregnation, reduces filling times, allows using lower pressure gradients (decreasing tooling costs), and permits using more viscous resins or resins with a faster reaction kinetics. However, by increasing the porosity the fiber volume fraction is decreased, which lowers composite final mechanical properties. Different fabrics have different curves of permeability versus porosity (or different n and C parameters) depending on the fiber type and fabric architecture.

When permeability is calculated using flow front position versus time data (during the impregnation of the dry preform) values of the unsaturated permeability K_{unsat} are obtained, while saturated permeability, K_{sat}, is obtained from volumetric flow rate data after the complete impregnation of the preform. The investigations made on synthetic fibers about the differences between these two permeabilities are not consistent, and a wide variety of results have been reported. Kim et al. [55] and Diallo et al. [56] found that the saturated permeability was always lower than the unsaturated permeability, while other authors obtained opposite results [57–61]. Also, results have been reported showing that the saturated and unsaturated permeabilities were almost equal [60]. These discrepancies are usually attributed to experimental issues that could modify the saturated and unsaturated permeability ratio, such as mold deflection, capillary effect, microscopic flow, fiber channeling, and air bubbles [59].

 DOI 10.1002/pc

TABLE 6. Empirical compaction models used in vegetable fiber fabrics.

Model	Expression	Fitting Parameters
Power Law	$\sigma = A(V_F)^n$	A, n
Exponential	$\sigma = y_1 e^{R_0 V_F} + y_0$	Y_0, y_1, R_0
Freundlich	$\sigma(V_F) = a(V_F)^{bV_F - c}$	a, b, c
Five term polynomial	$\sigma = P_1 V_F^4 + P_2 V_F^3 + P_3 V_F^2 + P_4 V_F + P_5$	P_1, P_2, P_3, P_4, P_5

Perhaps the most important issue regarding the permeability of plant fiber reinforcements is that this parameter is not a property of the reinforcing material as it is usually accepted for synthetic fiber reinforcements. For a given fiber type, reinforcement architecture and preform porosity, permeability of plant fiber fabrics changes if different test fluids are used. This was found by several authors, being the most accepted explanation that due to their chemical composition rich in cellulose, these fibers absorb fluid as the impregnation takes place, causing the fibers to swell and therefore reducing porosity of the preform (the size of open flow paths is decreased). Mantanis et al. [62] showed that plant fibers also swell by a significant amount when exposed to various organic liquids with different functional groups such as amines, alcohol and benzene rings. Since the thermosetting resins and bio resins used in LCM are organic liquids with similar molecular weights as well as similar functional groups, they are also expected to cause significant swelling to plant fibers during the manufacture of composites. In addition, it was suggested that a sink effect occurs as the fibers remove fluid from the main flow stream, delaying the front flow and therefore decreasing the measured value of permeability [18]. Fluid absorption continues until the fiber saturation point is reached from which no further liquid can be taken up by the fiber. In general, more polar fluids will enhance fiber swelling and will cause higher fabric permeability variations than less polar fluids. Umer et al. [31] characterized the permeability of wood fiber mats obtained by different manufacturing techniques, and they found that when using glucose syrup the permeability was lower than when using mineral oil. While the permeability values obtained for wood fiber mats depended on the test fluid used for the experiments, the type of test fluid was found to have no effect on permeability values of glass fiber continuous filament mat. Umer et al. [34, 63] have probed in other publications that the permeability of plant fiber reinforcements decreases as the infiltration with polar fluids process takes place. Francucci et al. [18] used a 22% V/V water glycerin solution as the test fluid and found both saturated and unsaturated permeabilities of jute woven fabrics to increase when a Polyhydroxybutyrate (PHB) coating was applied on the fibers decreasing their fluid absorption. They showed that fiber swelling is still present, in a lesser degree (about one quarter of the swelling found with the polar test fluid), when vinyl ester and phenolic resins commercial resins are used. In another publication, Francucci et al. [64] measured the unsaturated permeability of jute woven fabrics with SAE20 mineral oil (non-polar) and a 22% V/V water glycerin solution, and found that the permeability measured with the polar fluid was lower than the permeability measured with the non-polar fluid, for the whole range of fiber volume fraction studied.

Usually, permeability measurements are performed with test fluids that are cheaper, easier to clean and healthier for the operators than the polymeric resin that will be used during processing of the composite part. Therefore, permeability values obtained in laboratory conditions may lead to significant errors in the prediction of filling times and simulations of the mold filling stage. It is important to study the fluid-fiber interaction and assure that the swelling degree caused by the test fluid is equal to that of the one caused by the resin to be used during processing.

Many authors have measured the magnitude of permeability for different reinforcements made of natural fibers to probe their suitability for LCM processes. O'Donnell et al. [65] developed composites panels of soy oil-based resin and different natural fibers (flax, hemp and cellulose mats and recycled paper). They determined the permeability of the reinforcements and, except for the case of the recycled paper, the obtained values were high enough for infusing by vacuum assisted RTM (VARTM). Umer et al. [31] used diluted glucose syrup and mineral oil as test fluids and they found in both cases that wood fiber mats have permeability two orders of magnitude lower than glass fiber mats. According to the authors, using similar fiber volume fractions, wood fiber mats takes 100 times longer to fill for constant pressure injection, and if constant flow rate injection is applied, the required injection pressure will increase by 100 times. Khoun et al. [32] compared the saturated and unsaturated permeability of chopped strands mats flax and hemp fiber mats with that of discontinuous glass chopped strands fiber mat. They found both saturated and unsaturated permeabilities of the glass mat to be almost one order of magnitude higher than that of the hemp and flax mats at low fiber volume fractions (about 0.2). As the fiber content was increased, the difference between the glass and cellulosic fiber mats was found to decrease significantly.

Umer et al. [37] demonstrated that varying the yarn diameters and lengths has a significant influence on the permeability of mat style plant fiber LCM reinforcements. They found large yarn diameter mats to have 68 to 79% lower permeability as compared to the medium and small yarn diameter mats, which was attributed to the difference in surface structure and amount of twist present in the yarn. The mats manufactured from the 50 mm yarn length had higher permeability at higher fiber contents as compared to the 15 mm yarn length mats, while at lower fiber contents they did not find any difference. They hypothesized that

TABLE 7. Unsaturated permeability data of some vegetable fiber fabrics and mats.

Fiber/Fabric	Test fluid	Procedure	Experimental fiber volume fraction range	Carman Kozeny parameters		K_{unsat}			Ref
				n	*C*	$V_F = 0.2$	$V_F = 0.3$	$V_F = 0.4$	
Jute/woven fabrics 330 g/m^2	22% V/V water/glycerin solution	Constant pressure experiments	0.2–0.45	1.29	1.34 E+10	3.57 E−10	1.56 E−10	7.56 E−11	8
Jute/woven fabrics 330 g/m^2	Vinyl ester resin		0.26–0.39	1.84	3.04 E+10	3.39 E−10	1.10 E−10	4.17 E−11	75[b]
Jute/woven fabrics 330 g/m^2	SAE 20 Motor Oil		0.25–0.5	1.95	2.54 E+10	4.73 E−10	1.44 E−10	5.22 E−11	64
Sisal/random mat. 850 g/m2	12% V/V water/glycerin solution		0.2–0.46	1.48	4.80 E+08	1.30 E−08	5.11 E−09	2.28 E−09	54
Jute/woven fabrics 330 g/m^2			0.25–0.4	1.48	5.30 E+08	1.17 E−08	4.63 E−09	2.06 E−09	
Hemp/strand mat. 500 g/m^2	Silicone oil		0.16–0.5	1.56	2.44 E+10	2.86 E−10	1.08 E−10	4.63 E−11	32[b]
Flax/strand mat 500 g/m^2			0.16–0.6	1.37	2.38 E+10	2.26 E−10	9.42 E−11	4.40 E−11	
Recycled paper/mat 110 g/m^2	Not reported	Constant flow rate experiments	Single value: 0.423	–	–	–	–	3.60 E−13[a]	65
Flax/mat			Single value: 0.31			–	1.02 E−10[a]	–	
Cellulose/mat 200 g/m^2			Single value: 0.183			6.00 E−10[a]	–	–	
Chemically treated pulp/mat			Single value: 0.292			–	3.12 E−10[a]	–	

[a]These values were calculated by the authors for the single value of fiber volume fraction reported. Therefore, they do not exactly match fiber volume fractions of 02. 0.3, and 0.4.

[b]Carman Kozeny parameters were not provided by the authors, but calculated in this work from permeability vs. fiber volume fraction data reported in each paper.

the observed difference was due to the lower influence the ends have for the larger bundle lengths, because bundles untwist at the ends, allowing filaments to spread out, filling the open flow channels available for resin flow.

One of the most widely used chemical treatments performed on natural fiber fabrics in order to improve their composite properties is mercerization (alkali treatment) [66–73]. Due to the chemical and microstructural changes suffered by the fibers upon mercerization fabric permeability could also be affected. Rodriguez et al. [74] manufactured composites reinforced with alkali treated and untreated jute woven fabrics. They found that the infiltration time of the untreated fabrics was shorter than that of the treated ones. They suggested that alkali treatment decreases fabric permeability because it removes the coatings that are added to facilitate the woven/weaving procedure (potato starch and waxes) and the fiber surface became rougher. In addition authors claimed that fiber fibrillation, i.e., axial splitting of the elementary fibers (or microfibers) occurs and fiber diameter decreases during the treatment, increasing the exposed area and therefore the flow resistance.

All the experimental results presented in this section agree that the permeability of plant fiber reinforcement is dependent of the fluid that is being injected because these fibers absorb fluid and swell, causing the porosity and permeability of the preform to decrease as the infiltration takes place.

Tables 7 and 8 summarize unsaturated and saturated permeability values found in literature for different types of natural fiber reinforcements. The test procedure and test fluid used in the measurements are specified. Permeability values for fiber volume fractions of 0.2, 0.3, and 0.4 were calculated with the Carman–Kozeny model, which parameters are also presented in the tables. A permeability database containing a set of results from carefully controlled measurements for both saturated and unsaturated flows in glass fabrics can be found in Ref. 75. In this article, authors found the permeability of different glass fiber fabrics to be in the range 5E-9 to 2E-12 for fiber contents between 20 and 55% respectively. It can be seen in Tables 7 and 8 that plant fiber fabrics permeability values are very similar to those found for glass fabrics. This means that the time needed for impregnation of plant fiber fabrics should be the same than in glass fiber fabrics, if swelling effects are not significant and the same resin viscosity and injection pressure are used.

Current Models for the Impregnation Stage of Plant Fiber Reinforcements

As it was stated in the beginning of Impregnation of Plant Fiber Fabrics section, Darcy's law is used in

 DOI 10.1002/pc

TABLE 8. Saturated permeability data of some vegetable fiber fabrics and mats.

Fiber/Fabric	Test fluid	Procedure	Experimental fiber volume fraction range	Carman–Kozeny parameters		K_{sat}			Refs.
				n	C	$V_F = 0.2$	$V_F = 0.3$	$V_F = 0.4$	
Jute/woven fabrics 330 g/m^2	22 % V/V water/glycerin solution	Constant pressure experiments	0.2–0.45	0.91	8.46 E+09	3.36 E−10	1.80 E−10	1.03 E−10	8
Sisal/random mat, 850 g/m^2			Single value: 0.2	–	–	2.10 E−09	–	–	33
Wood/random mat (DMF)[a], 350–375 g/m^2	Glucose syrup/ water solution		0.2-0.4	2.21	9.27 E+11	1.86 E−11	4.93 E−12	1.59 E−12	31[e]
Wood/random mat (MDF)[b], 2000–2100 g/m^2				3.40	5.52 E+12	1.61 E−11	2.26E-12	4.31 E−13	
Wood/random mat (HS)[c], 400 g/m^2				2.26	1.76 E+12	1.04 E−11	2.69 E−12	8.52 E−13	
Wood/random mat (PDF)[d], 400 g/m^2				3.58	7.73 E+12	1.49 E−11	1.89 E−12	3.32 E−13	
Wood/random mat (HS), 400 g/m^2	Mineral oil			1.81	6.83 E+11	1.44 E−11	4.75 E−12	1.83 E−12	
Wood/random mat (MDF), 2000–2100 g/m^2				1.74	3.30 E+11	2.69 E−11	9.23 E−12	3.68 E−12	
Wood/random mat (DMF), 350–375 g/m^2				1.80	2.46 E+11	3.94 E−11	1.31 E−11	5.06 E−12	34
Wood/random mat (PDF), 400 g/m^2				1.76	4.00 E+11	2.29 E−11	7.77 E−12	3.06 E−12	
Flax/mat, 400 g/m^2 (small diameter, short length yarn)				2.19	1.05 E+10	1.59 E−09	4.27 E−10	1.39 E−10	37[e]
Flax/mat, 400 g/m^2 (small diameter, long length yarn)				2.04	8.01 E+09	1.68 E−09	4.91 E−10	1.71 E−10	
Flax/mat, 450 g/m^2 (large diameter, short length yarn)				2.35	4.28 E+10	4.85 E−10	1.20 E−10	3.64 E−11	
Flax/mat, 450 g/m^2 (large diameter, long length yarn)				2.33	2.90 E+10	6.98 E−10	1.74 E−10	5.33 E−11	
Hemp/strand mat, 500 g/m^2	Silicone oil		0.16–0.5	1.28	1.74 E+10	2.73 E−10	1.20 E−10	5.82 E−11	32[e]
Flax/strand mat, 500 g/m^2			0.16–0.6	1.51	1.83 E+10	3.54 E−10	1.37 E−10	6.04 E−11	

[a]Dry mat former.
[b]Medium density fiber mats.
[c]Hand sheets.
[d]Paper dynamic former mats.
[e]Carman Kozeny parameters were not provided by the authors, but calculated in this work from permeability vs. fiber volume fraction data reported in each paper.

modeling flow processes in composite materials manufacturing. In addition, if no sinks or sources of fluid exist throughout the mold being filled, the continuity equation should be also used to describe the fluid flow. The expression for the one-dimensional continuity equation is:

$$\frac{\partial}{\partial x}(\overline{u_x})=0 \tag{4}$$

Merging the continuity equation with Darcy's law:

$$\frac{\partial}{\partial x}\left(\frac{K}{\phi\eta}\frac{\partial P}{\partial x}\right)=0 \tag{5}$$

which means that the pressure distribution along the wetted region of the preform follows a linear behavior. The relationship between the pressure and the position of the flow front can be found if appropriate boundary conditions are established at the inlet and outlet resin ports.

As it was explained before, the permeability of plant fiber preforms changes with time if swelling fluids such as the case of water based resins, are used in the processing of the composites. The increase in fiber diameter reduces the porosity of the preform, and therefore its permeability. This process continues as the infiltration takes place until the saturation time is reached, which is different for each natural fiber type.

Some models accounting for the variable permeability of plant fiber fabrics have been developed and can be found in literature. Masoodi and Pillai [76, 77] proposed different approaches to model the mold filling process when plant fibers are used as reinforcement. They obtained good results by assuming that the permeability of the wetted region of the preform to be a function of time exclusively. This means that the permeability value is uniform in the entire wetted part of the preform, and it changes with time as the injection proceeds. Therefore, solving Darcy's law accounting for these considerations, the authors suggested the following equation to predict the position of the flow front with time during one dimensional infiltration:

$$x_f=\sqrt{\frac{2p_{\text{in}}}{\varepsilon_0\eta}\int_0^t K(t)dt} \tag{6}$$

where p_{in} is the injection pressure, η is the resin viscosity, $K(t)$ is the time-dependent global permeability of the wetted fiber mats behind the moving resin-front and ε_0 is the surface porosity at the liquid front, which incidentally is the initial porosity of fiber mats before swelling. Then, the authors proposed a linear relationship between the permeability of the wetted preform and time, as shown in *Eq. 7*.

$$K(t)=K_0+\frac{K_{\text{end}}-K_0}{t_{\text{end}}}t \tag{7}$$

Permeability tests were performed with a nonswelling fluid to estimate the K_0 and with the swelling fluid to obtain K_{end}. Despite the simple relationship proposed between the permeability and time, the results obtained by the mentioned authors were acceptable, and they were more accurate than the ones obtained by neglecting the fluid absorption and fiber swelling effect on the permeability.

Francucci et al. [64] proposed another approach considering that the permeability remains constant for a given value of porosity and what changes is precisely the free space for fluid flow throughout the preform. They related permeability and time by using the Carman-Kozeny model (*Eq. 3*), and considering the porosity as a function of time. They claimed that the model parameters, n and C, should be estimated from a permeability versus porosity curve obtained from permeability tests performed with a non-swelling fluid. In addition, the change in porosity with time was calculated from swelling curves (fiber diameter vs. time) with *Eq. 8*, where ϕ_0 is the porosity of the dry perform and $D_f(t)/D_{f_0}$ is the ratio between the instantaneous fiber diameter and the dry fiber diameter.

$$\phi(t)=1-(1-\phi_0)\left(\frac{D_{\text{f}}(t)}{D_{\text{f}_0}}\right)^2 \tag{8}$$

Authors fitted the change in diameter with time with an exponential function as suggested by Masoodi and Pillai [76]. Such a function has three empirical parameters, a, b, and c. Finally, the expression for predicting the flow front position resulted:

$$x_{\text{f}}=\sqrt{\frac{2P_{\text{in}}}{\eta C}\int\frac{\left\{1-(1-\phi_0)\left[a\exp\left(\frac{b}{c+t}\right)\right]^2\right\}^{n+1}}{\left\{(1-\phi_0)\left[a\exp\left(\frac{b}{c+t}\right)\right]^2\right\}^{n}}dt} \tag{9}$$

This model was named by the authors as the homogeneously variable permeability model (HVPM) and, such as the one proposed by Masoodi and Pillai [76], considers that the entire wetted region of the reinforcement has the same porosity (or permeability) at any given time since the fluid reached the beginning of it.

Another model proposed by Francucci et al. [64], called permeability field model (PFM), takes into account the fact that the zones of the wetted preform located more distant to the flow front remained immersed in the fluid longer than the zones of the wetted preform located closer to the front. This means that the degree of fiber swelling changes along the length of the wetted preform, leading to a field of porosities and permeabilities. Authors used Darcy's Law and the movement of the flow front was modeled with the technique called "Volume of fluid" (VOF), which uses the velocity field and a fully convective scheme with SUPG stabilization [78, 79]. The model was solved using the finite element method. An interesting fact found in the model results was that despite the pressure drop is linear within each element of the mesh; the global pressure distribution did not follow a linear behavior, instead of the models that consider a constant

 DOI 10.1002/pc

permeability value in the wetted region of the preform. This is because each element of the mesh has its own permeability value, being lower the permeability of the elements closer to the resin inlet gate than that of the elements closer to the flow front.

All models that took into account the swelling of the fibers predicted a much slower flow front movement that the model that assumes that permeability is constant over time and were more accurate in predicting the fluid flow through the preform when swelling fluids were used. The permeability field model predicted a greater flow rate than the homogeneously variable permeability model, but this difference in the velocity field was observed to be small and to occur only during a certain time range.

Summarizing, all the models mentioned in this section can be used with good accuracy to predict the mold filling stage when a swelling fluid is going to be used to impregnate plant fiber fabrics. The model proposed by Masoodi and Pillai [76] is a very simple and accurate model that needs permeability tests to be performed with a swelling and a non-swelling fluid in order to obtain the parameters of the model. This should be repeated every time the initial (dry) porosity of the preform is changed. Another simple model, the homogeneously variable permeability model (HVPM), was proposed by Francucci et al. [64], in which a single permeability vs. porosity curve is needed, measured with a non-swelling fluid, and then the model parameters are extracted from swelling tests performed with the fluid to be injected into the mold. The most complex model, the permeability field model, accounts for different permeabilities throughout the preform as different zones were immersed different periods of time. Although this model is more complex to use numerically, the experimental requirements to obtain the parameters are exactly the same as in the HVPM.

Capillary Effects During the Impregnation of Plant Fiber Fabrics

Reinforcements made by waving or stitching fiber bundles have dual scale porosity. This means that micro pores exist between fibers comprising the bundles, and macro pores exist between the bundles. Therefore, a dual scale flow occurs and the micro flow can be affected by capillary pressure. Capillary effects have shown to be determinant in the mechanism of void formation during infiltration of fabrics [80–84]. These voids remain in the composite microstructure as residual porosity after the resin cures, having a detrimental effect on the mechanical performance of the material. Capillary pressure is also important at low impregnation rates since it acts as the driving force for the impregnation of the reinforcement [85].

Capillary effects during the impregnation of jute woven fabrics were studied by Francucci et al. [86]. The authors measured the capillary pressure drop developed at the flow front during infusion of jute woven fabric with a water/glycerin solution and vinyl ester resin, using the methods proposed by Verrey et al. [87]. They found the capillary pressure to be negative, i e. enhancing flow, when the water/glycerin solution was used due to the polar nature this fluid that makes it very compatible with the hydroxyl groups at the fiber's surface. On the other hand, the lower polar nature of the vinyl ester resin leaded to positive values of capillary pressure, i e. opposed to flow. The magnitude of the capillary effects was significant, about 20% of the external applied pressure when the water/glycerin fluid was injected and 35% when the vinyl-ester resin was used. Since capillary pressure is not taken into account for the permeability tests, this difference in the capillary pressure sign led to an increase of the measured fabric permeability when the polar test fluid was injected and a lower permeability value when vinyl ester resin was used, in contrasts with what was expected because of the fiber swelling effect. The authors also found that capillary pressure increased with fiber volume content. The magnitude of capillary pressure in jute fiber fabrics was found to be two to three times higher than the reported for synthetic fibers. The authors explained this difference stating that the hollow and imperfect structure of plant fibers provides more capillary channels in which micro flow can occur.

CONCLUSIONS

Natural fibers, particularly plant fibers, are being used as a replacement of glass fibers in many applications. However, one of the keys of its success is the possibility of using the traditional composites processing techniques, like RTM, VI or other liquid composite molding method. Therefore, it is crucial to understand how the main processing variables are affected when glass fibers are replaced by natural fibers, which have different structure, different fabric architecture and different chemical interactions with the resins. This knowledge will allow manufacturing high quality green composite parts.

The first stage of any LCM process is the compaction of a stack of fabric layers inside the mold cavity. The main findings regarding the compaction of plant fiber preforms are:

- Plant fiber preforms are harder to compress than glass fiber preforms, due to their rough surface morphology and lack of fiber alignment in the bundles. This means that large clamping forces are needed to achieve high fiber contents. In addition, low fiber volume fractions are obtained if the vacuum infusion technique is used, which has a maximum compaction pressure of 1 atm.
- The permanent deformation experienced by plant fiber preforms during the compaction stage is higher than the experienced by glass fiber preforms. This was attributed to the hollow structure of plant fibers that collapses as the laminate thickness is reduced and the fiber content is increased. This means that higher fiber contents are

achievable if a pre-forming step is carried out by applying one or more compressive loading cycles prior to the compaction stage of the processing technique.
- Plant fibers soften due to the absorption of polar fluids, such as water based resins and bio resins, decreasing the compaction pressure needed to achieve a certain fiber volume fraction.

After compressing the fabric layers, resin is forced to flow through the dry reinforcement. The main findings about the issues arise during impregnation of plant fiber fabrics are:

- When using polar fluids, fluid absorption and saturation of natural fibers cause fiber swelling, reducing the porosity and increasing flow resistance. In addition, the fluid is removed from the main stream as it travels through the reinforcement and thus decreasing flow velocity during the unsaturated flow. These factors reduce the permeability of the preform. Therefore, permeability values measured with water based or polar test fluids will lead to significant errors in the prediction of filling times and flow patterns. Permeability should be measured with the same resin that will be used during the real manufacturing process, or a very similar fluid in terms of polarity and chemical composition.
- In fabrics with dual scale porosity, capillary pressure may be significant when plant fibers are used, because the hollow and imperfect structure of these fibers provides capillary channels in which micro flow can occur. Polar fluids are very compatible with the hydroxyl groups at the fiber's surface, causing a capillary pressure that enhances flow, while fluids with low polarity can lead to capillary pressure that opposes flow.

Different models were developed in literature for simulating of the mold filling stage of plant fiber composites, accounting for the variation in permeability caused by fiber swelling. Those models predicted the flow front movement with very good accuracy when swelling fluids were used in permeability experiments. All the proposed models require swelling curves (plots relating fiber diameter with time) or permeability tests for the fiber-fluid system to be modeled. The development of a simpler procedure to determine fiber swelling when exposed to different fluids could ameliorate the simulation of LCM with plant fibers.

On the other hand, models that consider a constant value of permeability were accurate in predicting flow front position only when non-swelling fluids were used. If swelling fluids were used, constant permeability models overestimate the position of the flow front.

REFERENCES

1. M. Miao and N. Finn, *J. Text. Eng*., **54**, 6 (2008).
2. V.K. Thakur, *Green Composites from Natural Resources*, CRC Press Taylor & Francis, Boca Raton, Fl, USA, (2013).
3. C. Baley. *Compos. A*, **33**, 7 (2002).
4. N. Reddy and Y. Yang, *Trends Biotechnol*., **23**, 1 (2005).
5. K.G. Satyanarayana, J.L. Guimarães, F. Wypych, *Compos. A*, **38**, 7 (2007).
6. M.J. John and R.D. Anandjiwala, *Polym. Compos*., **29**, 2 (2008).
7. J. Biagiotti, D. Puglia,and J.M. Kenny, *J. Nat. Fiber*., **1**, 2 (2004).
8. P. Mallick, "Glass fibers," in *Fiber Reinforced Composites: Materials, Manufacturing, and Design*, P. Mallic, Ed., Taylor & Francis Group, Boca Raton, FL (2007).
9. C Scarponi, *Industrial Applications for Natural-Fibre-Reinforced Composites*, JEC Composites Magazine, Paris (2009).
10. D. Nabi Saheb and J.P. Jog, *Adv. Polym. Technol*., **18**, 4 (1999).
11. P. Wambua, J. Ivens, and I. Verpoest, *Compos. Sci. Technol*., **63**, 9 (2003).
12. T. Corbière-Nicollier, B. Gfeller Laban, L. Lundquist, Y. Leterrier, J. A. E. Månson, and O. Jolliet, *Resour. Conserv. Recycle*, **33**, 4 (2001).
13. S.V. Joshi, L.T. Drzal, A.K. Mohanty, and S. Arora., *Compos A*, **35**, 3 (2004).
14. W.P. Schmidt and H.M. Beyer, *SAE Trans*., **107**, 6 (1998).
15. K. Wötzel, R. Wirth, and M. Flake, *Angew. Makromol. Chem*., **272** (1999).
16. R. Zah, R. Hishier, A.L. Leão, and I. Braun, *J. Clean. Prod*., **15**, 11 (2007).
17. R. Rowell, A.R. Sanadi, D. Caulfield, and R. Jacobson, "Utilization of natural fibers in plastic composites: problems and opportunities," in A.L. Leao, F.X. Carvalho, E. Frollini, Eds., *Lignocelulosic Plastics—Composites*, USP and UNESP, San Pablo (1997).
18. G. Francucci, E.S. Rodríguez, and A. Vázquez, *Compos. A*, **41**, 1 (2010).
19. J. Bréard, Y. Henzel, F. Trochu, and R. Gauvin, *Polym. Compos*., **24**, 3 (2003).
20. H. Burger, A. Koine, R. Maron, and K. Mieck, *Polym. Sci. Technol*., **22**, 8 (1995).
21. N.M. Everitt, N.T. Aboulkhair, and M.J. Clifford, "Looking for links between natural fibres' structures and their physical properties," in *Proceedings of International Conference on Natural Fibers*-Sustainable *Materials for Advanced Applications*, Guimarães (2013), 9-11 June 2000.
22. W.D. Brouwer, "Natural fibre composites in structural components: alternative applications for sisal?" in *Proceedings of a Seminar held by the Food and Agriculture Organization of the UN (FAO) and the Common Fund for Commodities (CFC)* (2000), December 13.
23. S. Advani and E. Sozer Murat, Process *Modeling in Composites* Manufacturing, Marcel Dekker, New York (2003).
24. M. O. W. Richardson and Z.Y. Zhang, *Compos. A*, **31**, 12 (2000).
25. N. P. J. Dissanayake, J. Summerscales, S. M Groove, and M.M. Singh, "Infusion of natural vs. synthetic fibre composites with similar reinforcement architecture in the context of an LCA," in *Proceedings of FPCM-9 Conference,* Montreal, Canada (2008), 7-9 July 2008.

 DOI 10.1002/pc

26. B. Chen, E.J. Lang, and T. W Chou, *Mater. Sci. Eng. A*, **317**, 1 (2001).
27. J. Breard, Y. Henzel, F. Trochu, and R. Gauvin, *Polym. Comp.*, **24**, 3 (2003).
28. P.A. Kelly, R. Umer, and S. Bickerton, *Compos. A*, **37** (2006).
29. A.A. Somashekar, S. Bickerton, and D. Bhattacharyya, *Compos. A*, **37** (2006).
30. F. Robitaille and R. Gauvin, *Polym. Compos.*, **20**, 1 (1999).
31. R. Umer, S. Bickerton, and A. Fernyhough, *Compos. A*, **38**, 2 (2007).
32. L. Khoun, F. Busnel, and D. Maillard, "Compaction behaviour and permeability of cellulosic fibre for RTM applications," in *Proceedings of SPE Automotive Composites Conference & Exhibition*. Michigan (2013), 11-13 September, 2013.
33. G. Francucci, A. Vázquez, and E.S. Rodríguez, *Text. Res. J.*, **82**, 17 (2012).
34. R. Umer, S. Bickerton, and A. Fernyhoug, *Compos. A*, **39**, 624 (2008).
35. B. Madsen and H. Lilholt, "Compaction of plant fibre assemblies in relation to composite fabrication. Sustainable natural and polymeric composites–science and technology," in *Proceedings of the 23rd Risoe International Symposium on Materials Science,* Roskilde (2002), 2-5 September, 2002.
36. G. Francucci, A. Vázquez, and E.S. Rodríguez, *J. Compos. Mater.*, **46**, 155 (2012).
37. R. Umer, S. Bickerton, and A. Fernyhough, *Compos. A*, **42**, 723 (2011).
38. L. Lundquist, F. Willi, Y. Leterrier, and J. A. E. Manson, *Polym. Eng. Sci.*, **44**, 45 (2004).
39. C. Poilâne, Z.E. Cherif, F. Richard, A. Vivet, B. Ben Doudou, and J. Chen, *Compos. Struct.*, **112**, 100 (2014).
40. C. A Lenth and F.A. Kamke, *Wood Fiber Sci.*, **33**, 3 (2001).
41. B. Chen, E.J. Lang, and T. W Chou, *Mater. Sci. Eng. A*, **317**, 1 (2001).
42. B. Chen and T.W. Chou, *Compos. Sci. Technol.*, **59**, 10 (1999).
43. J. Bréard, Y. Henzel, F. Trochu, and R. Gauvin, *Polym. Compos.*, **24**, 3 (2003).
44. P. Potluri and T.V. Sagar, *Compos. Struct.*, **86**, 1 (2008).
45. B. Chen, A. H. D Cheng, and T.W. Chou, *Compos. A*, **32**, 5 (2001).
46. B. Chen and T.W. Chou, *Compos. Sci. Technol.*, **60**, 12 (2000).
47. T.G. Gutowski, Z. Cai, S. Bauer, D. Boucher, J. Kingery, and S. Wineman, *J. Compos. Mater.*, **21**, 7 (1987).
48. S. Toll, *Polym. Eng. Sci.*, **38**, 8 (1998).
49. P Šimáček and V.M. Karbhari, *J. Reinf. Plast. Comp.*, **15**, 1 (1996).
50. Z. R Chen and L. Ye, *Compos. Sci. Technol.*, **66**, 16 (2006).
51. Z.R. Chen, L. Ye, and T. Kruckenberg, *Compos. Sci. Technol.*, **66**, 16 (2006).
52. G. Francucci and E.S. Rodríguez, *J. Appl. Polym. Sci.*, **124** (2012).
53. C.H. Shih and J. Lee, *Polym. Compos.*, **19**, 5 (1998).
54. E. Rodriguez, F. Giacomelli, and A. Vázquez, *J. Compos. Mater.*, **38**, 3 (2004).
55. Y.R. Kim, S. P McCarthy, J.P. Fanucci, S.C. Nolet, and C. Koppernaes, *SAMPE Quart.*, **22**, 3 (1991).
56. M.L. Diallo, R. Gauvin and F. Trochu, "Key factors affecting the permeability measurement in continuous fiber reinforcements." in Proceedings of 23rd International Conference on Composite Materials, Gold Cost, Australia (1997), 14-18 July, 1997.
57. T.S. Lundström, R. Stenberg, R.Bergstrom, H. Partanen, and P.A. Birckeland, *Compos. A*, **31**, 1 (2000).
58. F.M. Foley and T. Gutowski, "The effect of process variables on permeability in the flexible resin transfer molding (FRTM) process," in *Proceedings of 23rd International SAMPE Technical Conference,* Kiamesha Lake (1991), 21-24 October, 1991.
59. A. Shojaei, F. Trochu, S.R. Ghaffarian, S. M. H. Karimian, and L. Lessard, *J. Reinf. Plast. Comp.*, **23**, 4 (2004).
60. Y. Lai, H.B. Khomami, and J.L. Kardos, *Polym. Compos.*, **18**, 3 (1997).
61. K. Pillai and S.A. Advani, *J. Compos. Mater.*, **32**, 19 (1998).
62. G.I. Mantanis, R.A Young, and R.M. Rowell, *Cellulose*, **2**, 1 (1995).
63. R. Umer, S. Bickerton and A. Fernyhough, "Chapter 23: Wood fiber mats as reinforcements for thermosets," in *Engineering Biopolymers: Homopolymers, Blends and Composites*, S. Fakirov, D. Bhattacharya D, Eds., Hanser, Munich (2007).
64. G. Francucci, E. Rodriguez, and J. Moran, *J. Compos. Mater.*, **48**, 2 (2014).
65. A. O'Donnell, M.A. Dweib, and R.P. Wool, *Compos. Sci. Technol.*, 64 (2004).
66. I. Van de Weyenberg, J. Ivens, B. De Coster, B. Kino, E. Baetens, and I. Verpoest, *Compos. Sci. Technol.*, **63**, 9 (2003).
67. Gañan and S. Garbizu, R. Llano-Ponte and I. Mondragon, *Polym. Compos.*, **26**, 2 (2005).
68. T. H. D. Sydenstricker, S. Mochnaz, and S.C. Amico, *Polym. Test.*, **22**, 4 (2003).
69. M.Z. Rong, M.Q. Zhang, Y. Liu, Z.W. Zhang, G.C. Yang, and H.M. Zeng, *Compos. Sci. Technol.*, **61**, 10 (2001).
70. D. Ray, B.K. Sarkar, and N.R. Bose, *Compos. A*, **33**, 2 (2002).
71. D. Ray, B.K. Sarkar, S. Das, and A.K. Rana, *Compos. Sci. Technol.*, **62**, 7 (2002).
72. A.C. Albuquerque, K. Joseph, L. Hecker de Carvalho, and J.R. Morais d'Almeida, *Compos. Sci. Technol.*, **60**, 6 (2000).
73. J. Gassan and A.K. Bledzki, *Compos. Sci. Technol.*, **59**, 9 (1999).
74. E.S. Rodriguez, P.M. Stefani, and A. Vazquez, *J. Compos. Mater.*, 41 (2007).
75. R.S. Parnas, K.M. Flynn, and M. E. A. Dal-Favero, *Polym. Compos.*, **18**, 5 (1997).
76. R. Masoodi and K.M. Pillai, "Modeling the processing of natural fiber composites made using liquid composite molding," in *Handbook of Bioplastics* and Biocomposites Engineering Applications, K.M. Pillai, Ed., John Wiley & Sons, Inc., New York (2011).

77. R. Masoodi and K.M. Pillai, *AICHE J*., **56**, 9 (2010).
78. C.W. Hirt and B.D. Nichols, *J. Comput. Phys*., **39**, 1 (1981).
79. T. J. R. Hughes, The Finite Element Method: Linear Static and Dynamic Finite Element Analysis, Dover Publications, New York (2000).
80. N. Patel and L.J. Lee, *Polym. Compos*., **17**, 96 (1996).
81. N. Patel and L.J. Lee, *Polym. Compos*., **17**, 104 (1996).
82. N. Patel, V. Rohatgi, and L.J. Lee, *Polym. Eng. Sci*., **35**, 10 (1995).
83. G.L. Batch, Y.T. Chen, and C.W. Macosko, *J. Reinf. Plast. Compos*., **15**, 10 (1996).
84. C. Binetruy, J. Pabiot, and B. Hilaire, *Polym. Compos*., **21**, 4 (2000).
85. S. Amico and C. Lekakou, *Compos. Sci. Technol*., **61**, 13 (2001).
86. G. Francucci, E.S. Rodríguez, E. Ruiz, and A. Vázquez, *Polym. Compos*., 33 (2012).
87. J. Verrey, V. Michaud, and J. A. E. Månson, *Compos. A*, **37**, 1 (2006).

 DOI 10.1002/pc